European Neuropsychopharmacology (2019) 29, 1464–1475

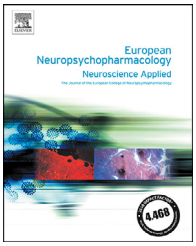

www.elsevier.com/locate/euroneuro

Methylation in *Syn* and *Psd95* genes underlie the inhibitory effect of oxytocin on oxycodone-induced conditioned place preference

Xin-Yu Fan[a], **Guang Shi**[b], **Ping Zhao**[a,*]

[a] *Department of Anesthesiology, Shengjing Hospital of China Medical University, No. 36 Sanhao Street, 110004, Shenyang, China*
[b] *Department of Neurology, Liaoning Provincial People's Hospital, Shenyang, China*

Received 3 July 2019; received in revised form 2 October 2019; accepted 29 October 2019

KEYWORDS
DNA methylation;
Oxycodone;
Oxytocin;
Synaptic proteins

Abstract
Oxycodone (Oxy) is one of the most effective analgesics in medicine, but is associated with the development of dependence. Recent studies demonstrating epigenetic changes in the brain after exposure to opiates have provided an insight into possible mechanisms underlying addiction. Oxytocin (OT), an endogenous neuropeptide well known for preventing drug abuse, is a promising pharmacotherapy to counteract addiction. Therefore, we explored the mechanism of Oxy addiction and the role of OT in Oxy-induced epigenetic alterations. In this study, drug-induced changes in conditioned place preference (CPP), i.e. the expression of synaptic proteins and synaptic density in the ventral tegmental area (VTA) were measured. We also sought to identify DNA methyltransferases (DNMTs), ten-eleven translocations (TETs), global 5-methylcytosine (5-mC), and DNA methylation of two genes implicated in plasticity (*Synaptophysin, Syn; Postsynaptic density protein 95, Psd95*). Oxy (3.0 mg/kg, i.p.) induced CPP acquisition in Sprague-Dawley rats. Oxy down-regulated DNMT1 and up-regulated TET1-3, leading to a decrease in global 5-mC levels and differential demethylation at exon 1 of *Syn* and exon 2 of *Psd95*. These changes in DNA methylation of *Syn* and *Psd95* elevated the expression of synaptic proteins (SYN, PSD95) and synaptic density in the VTA. Pretreatment with OT (2.5 μg, i.c.v.) via its receptor specifically blocked Oxy CPP, normalized synaptic density, and regulated DNMT1 and TET2-3

Abbreviations: aCSF, artificial cerebrospinal fluid; Ato, atosiban; CPP, conditioned place preference; DNMT, DNA methyltransferase; OT, oxytocin; Oxy, oxycodone; TET, ten-eleven translocation; VTA, ventral tegmental area; PSD95, post synaptic density protein 95; SYN, synaptophysin.

* Corresponding author.
E-mail address: zhaop@sj-hospital.org (P. Zhao).

https://doi.org/10.1016/j.euroneuro.2019.10.010

causing reverse of DNA demethylation of *Syn* and *Psd95*. DNA methylation is an important gene regulation mechanism underlying Oxy CPP, and OT – via its receptor – could specifically inhibit Oxy addiction.

1. Introduction

Oxycodone (Oxy) is a commonly used pain medication, and like many short-acting opioid agonists, it also has addiction potential (Remillard et al., 2019). Repeated administration of opiates produces functionally significant changes in neurobiological processes promoting reward-related learning and memory (van Steenbergen et al., 2019). Based on the extensive literature on opioid dependence and withdrawal, chronic opiates potently enhance glutamatergic and GABAergic function, and structural plasticity in the ventral tegmental area (VTA), a critical brain region involved in reward and motivation (Langlois and Nugent, 2017; Langlois et al., 2018). Drug-induced synaptic plasticity has attracted considerable interest in studies of drug addiction, as strong and durable memories associated with drug experience are demonstrated to promote compulsive drug taking and craving (Smaga et al., 2019). Synapses are the fundamental units of information transfer and memory storage in the brain, composed of presynaptic and postsynaptic compartments. Presynaptic proteins, such as SNAP-25 and synaptophysin (SYN), and postsynaptic proteins, such as homer 1 and post synaptic density protein 95 (PSD95), are reported to be modified by opiate use (Liu et al., 2016; Befort et al., 2010). However, the underlying molecular mechanisms of drug-induced changes in synaptic proteins are still not fully understood.

Several lines of evidence have suggested a key role for epigenetic modifications in forming and maintaining the addictive state (Dobs and Ali, 2019; Fiona et al., 2018). For example, DNA methylation (the covalent binding of a methyl group to cytosine to form 5-methylcytosine (5-mC)) aids the transition from active to repressed chromatin states, and is the most well-studied epigenetic mechanisms in the context of drug addiction (Lax et al., 2018). The DNA methylation landscape was shown to be altered by DNA methyltransferases (DNMTs) and ten-eleven translocations (TETs) in different animal models for opiates use (Wu et al., 2018; Sun et al., 2017). Members of the DNMT family including DNMT1, DNMT3A, and DNMT3B (Poetsch and Plass, 2011), along with TET methylcytosine dioxygenases (TETs including TET1-3) mediate the degradation of 5-mC, hence promoting DNA demethylation (Bian et al., 2014). The steady state of DNA methylation reflects a balance of methylation and demethylation (Detich et al., 2003). Differential methylation of the *bdnf* and opioid receptor Mu 1 gene have been reported in opiate-dependent individuals (Schuster et al., 2016; Marie-Claire et al., 2016). These phenomena thus lend further support to the notion that synaptic changes during opiate exposure may be mediated by altered DNA methylation.

In many species, the neuropeptide oxytocin (OT) is an important modulator of social and emotional processes, including reward, social stress, associative learning, memory and stress responses (Singh et al., 2016; Amini-Khoei et al., 2017). There is now strong evidence that OT is a key candidate for treating maladaptive processes associated with addiction (Stauffer et al., 2019; Zanos et al., 2017). OT attenuates cocaine-seeking and methamphetamine-primed reinstatement (Kohtz et al., 2018; Everett et al., 2018; Cox et al., 2016), as well as reducing opiate self-administration and decreasing craving and stress responses in marijuana-dependent individuals (McRae-Clark et al., 2013). Conversely, chronic methamphetamine/cocaine treatment was shown to cause an increase in plasma OT levels and OT receptor density in the amygdala (Georgiou et al., 2015a,2016, 2017; Baracz et al., 2016; Zanos et al., 2014a). A growing number of studies have also manipulated the acquisition, consolidation and retrieval process to disrupt memory by OT (Boccia et al., 1998; De Oliveira et al., 2007). Disrupting cue-drug memory consolidation is one of the most important strategies for reducing the strength of cues in motivating drug-seeking and -taking behavior (Sorg, 2012). However, the role of OT in Oxy-seeking behavior via persistent disruption of an established addictive memory and its underlying mechanism remain elusive. Therefore, the current study was designed to evaluate the effect of OT administration on Oxy conditioned place preference (CPP)-induced epigenetic alterations that underlie synaptic changes.

2. Methods

2.1. Animals

Adult male Sprague–Dawley rats, weighing 250–300 g, were purchased from BEIJING HFK BIOSCIENCE CO., LTD. All animals used for the conditioned place preference (CPP) experiment were group-housed (n = 2–3 per cage) and were maintained under standard conditions with a reversed 12 h:12 h light/dark cycle (lights on 8:00), controlled temperature (24 ± 1 °C), humidity (50 ± 10%), low noise, sufficient chow and water. After five days adaption, surgeries for implantation of intracerebroventricular cannula were conducted between 8:00 to 17:00 and behavioral test was performed between 8:00 to 12:00. All experimental procedures and protocols were approved by The Laboratory Animal Care Committee of China Medical University (2019PS130K), and were conducted according to the National Institutes of Health (NIH) Guide for the Care and Use of Laboratory Animals (NIH Publication No. 8023, revised 1978). Every effort was made to minimize animal suffering and the number of animals used.

2.2. Chemicals

Oxy (obtained from Shengjing Hospital of China Medical University) was dissolved in saline and injected intraperitoneally (i.p.) in a dose of 3.0 mg/kg. OT (Sigma, #o0770000) and Ato

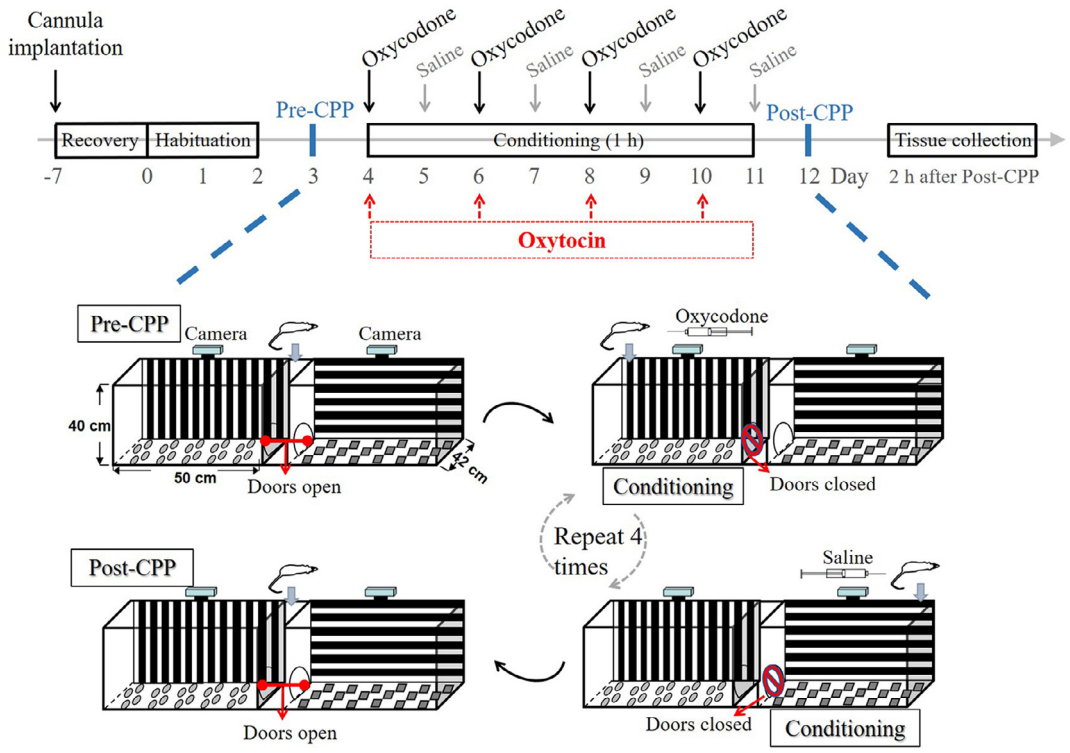

Fig. 1 A global timeline of the behavioral procedures. There were five animal groups for this experiment, namely Sal+aCSF ($n = 11$) as the control group, Oxy+aCSF ($n = 11$) as the model group, and Oxy+aCSF+OT ($n = 11$)/Oxy+aCSF+OT+Ato ($n = 11$)/Sal+aCSF+OT ($n = 11$) as the treatment groups. On even days (Days 4, 6, 8, 10), rats received either Oxy (3.0 mg/kg, i.p.) or saline at 30 min after OT (2.5 μg, i.c.v.) or aCSF administration. Ato (10.0 μg, i.c.v.), a competitive OT receptor antagonist, was administered 10 min before OT administration. On odd days (Days 5, 7, 9, 11), rats were given aCSF at 30 min before injection with saline. All rats underwent eight daily conditioning sessions for 1 h in the CPP chamber. On Day 12, the VTA was removed after post-CPP to observe the synaptic structures and the expression of SYN and PSD95. Finally, the DNA methylation status at exon 1 of *Syn* and exon 2 of *Psd95*, as well as expression levels of DNMTs and TETs were analyzed.

(Sigma, #a3480) were dissolved in aCSF composed of 145 mM NaCl, 2.8 mM KCl, 1.2 mM $CaCl_2$, 1.2 mM $MgCl_2$, 5.4 mM D-glucose, PH = 7.4 (all the solute purchased from Sigma, USA) with the concentration of 2.5 μg/μl and 10.0 μg/μl. OT and Ato were administered intracerebroventricularly (i.c.v.) in a volume of 1.0 μl/rat.

2.3. Behavioral procedures

Behavioral procedures were conducted in an isolated room with no disturbances during the tests. Rats in the CPP experiment ($n = 55$) were randomly distributed into the following groups: Saline+aCSF (Sal+aCSF; $n = 11$), Oxy+aCSF ($n = 11$), Oxy+aCSF+OT ($n = 11$), Oxy+aCSF+OT+Ato ($n = 11$; Ato, OT receptor antagonist), Saline+aCSF+OT (Sal+aCSF+OT; $n = 11$). Fig. 1 shows a global timeline of the behavioral procedures.

The CPP apparatus was made of opaque Plexiglass and consisted of two rectangular-based chambers (42 × 40 × 50 cm each) separated by a small room (20 × 10 × 50 cm) with two doors (10 × 14 cm). Eight groups of CPP chambers were used with an unbiased design, which featured distinct visual and tactile cues. The background of two chambers was different from each other, one was colored with alternating black and white transverse stripes (width 4 cm) on the wall with hollow quadrates in the floor, and the other had vertical stripes on the wall and hollow dots (diameter 1.0 cm) on the floor. A computer simultaneously operated the six devices that were enclosed in sound-attenuating cubicles. Time spent in each chamber and the track were calculated and analyzed using an Ethovision XT8.0 (Noldus information Technology, Wageningen, the Netherlands) computerized video tracking system.

The experimental design (shown in Fig. 1) included three phases: three daily habituation sessions, eight daily conditioning sessions and a final test session. During the first phase "pre-conditioning" (Days 1-2), rats were habituated to the apparatus and allowed to freely explore both chambers for 15 min. The pre-CPP test was carried out on Day 3, which meant that the time each rat spent in the two chambers was recorded automatically during a 15-min period. Animals that showed a strong unconditioned aversion or preference (less than 33% or more than 66% of the session time, i.e. 300 and 600 s, respectively) for either chamber were rejected. This approach of animal screening is commonly employed in cocaine/methamphetamine/morphine CPP (Maldonado et al., 2007; Qi et al., 2009; Hao et al., 2008). In the present study, 81 rats in total were used for animal screening, and 26 of them were excluded from the trial (11 rats with place aversion and 15 rats with place preference). During the second phase, animals underwent an experiment with an unbiased counterbalanced CPP design including eight daily conditioning sessions. On even days (Days 4, 6, 8, 10), rats received either Oxy (3.0 mg/kg) or saline 30 min after OT (2.5 μg/μl) or aCSF pretreatment. In the relevant group, Ato (10.0 μg/μl) was administered at 10 min before OT administration. All rats were confined for 1 h in the drug-paired chamber immediately after saline/Oxy injection. A dose of 3.0 mg/kg Oxy and 1 h confinement in the drug-paired chamber was chosen because it has been shown to induce 90-100% CPP in rats

(Ryan et al., 2018). The dose and time period of OT/Ato administration were chosen according to a previous report showing that OT (2.5 μg/μl, 30 min prior to each conditioning session) blocked the acquisition of methamphetamine CPP, and Ato (10.0 μg/μl, 10 min prior to OT administration) inhibited the effect of OT on methamphetamine CPP (Qi et al., 2009). Within each group, the drug-paired chamber was counterbalanced, so that half the rats were confined to the chamber with vertical stripes, while the rest were confined to the chamber with transverse stripes. This is an important step in the experimental procedure that avoids any preference bias before conditioning. On odd days (Days 5, 7, 9, 11), rats were given aCSF 30 min before saline injection and confined for 1 h in the opposite compartment (saline-paired chamber). In the third phase (Day 12), rats were placed in the apparatus and given free access to the two chambers for 15 min, and the time spent in each chamber was recorded.

2.4. I.c.v. injection

Surgical procedures for implantation of intracerebroventricular cannula were performed under anesthesia with isoflurane (Hebei YIPIN, China). A 26-gauge stainless-steel guide cannula was directed into the lateral cerebral ventricle (*A/P*−0.5 mm, *M/L* +1.5 mm, *D/V*−3.5 mm) unilaterally according to the atlas of Paxinos (Paxinos and Watson, 2013) and was fixed to the skull surface with dental cement. When the dental cement had hardened, a dummy cannula, cut to the same dimensions as the guide cannula, was inserted to seal the top of the guide cannula to prevent clogging and minimize possible risk of infection. The rats recovered for seven days before injection was made by inserting a 33-gauge stainless steel injector tube into the guide cannula. The injector tube was attached to a PE-10 tubing fitted to a 10-ml Hamilton syringe (Hamilton, NV, USA). One microliter of OT (2.5 μg/μl) or Ato (10 μg/μl) was infused into the lateral cerebral ventricle over five minutes by microinfusion pump.

2.5. Transmission electron microscopy (TEM)

The tissue was fixed in 1% osmium tetroxide/1.25% potassium ferrocyanide in 0.15 M sodium phosphate buffer for 1 h. Samples were dehydrated in a graded ethanol series, followed by propylene oxide, and were infiltrated and embedded in Polybed 812 resin (Polysciences). Ultrathin (70 nm) sections were taken, mounted on 200 mesh copper grids and stained with uranyl acetate and lead citrate. The ultrathin sections were observed and photographed using TEM (JEM-1200EX, Jeol Ltd., Tokyo, Japan) at an accelerating voltage of 80 kV. Images of synaptic structures were focused onto a fluorescent screen and processed with Adobe Photoshop (Adobe Systems Software, Ireland). Synapses were identified according to well-established criteria (Colonnier and Beaulieu, 1985). The synaptic density was measured quantitatively in the VTA based on methods described previously (DeFelipe et al., 1999).

2.6. Western blotting

The tissue was lysed with T-PER Tissue Protein Extraction Reagent (1:10, 10 μl reagent/1 mg tissue, Thermo Scientific, Rockford, USA), 0.1% phenylmethanesulfonyl fluoride (PMSF), 0.1% sodium fluoride (NaF), and 0.1% sodium orthovanadate (Na_3VO_4), sonicated for 3 min on ice with a probe sonicator and centrifuged for 15 min at 14,000 g at 4 °C, and then the supernatant was extracted and boiled in water bath. Protein extracts (30–50 μg) were separated by 10% sodium dodecyl sulfate-polyacrylamide gel electrophoresis (SDS-PAGE) and electrophoretically transferred to a nitrocellulose membrane at 4 °C. Blots were incubated for 1 h with 5% non-fat milk to block non-specific binding sites and then incubated with primary antibodies, including rabbit anti-SYN antibody (Abcam, #ab32127, 1:10000), rabbit anti-PSD95 antibody (Cell Signaling Technology, #3409S, 1:1000), rabbit anti-DNMT1 antibody (Abcam, #ab188453, 1:1000), rabbit anti-DNMT3A antibody (Abcam, #ab2850, 1:500), rabbit anti-DNMT3B antibody (Abcam, #ab2851, 1:500), rabbit anti-TET1 antibody (Abcam, #ab191698, 1:500), rabbit anti-TET2 antibody (Abcam, #ab124297, 1:250), rabbit anti-TET3 antibody (Abcam, #ab139805, 1:500) and mouse anti-GAPDH (Cell Signaling Technology, #51332, 1:10000) overnight at 4 °C, secondary antibodies for 1 h at room temperature. Protein bands were visualized by enhanced chemiluminescence and quantified with ImageJ software (NIH).

2.7. Quantification of the 5-methylcytosine level in DNA

Genomic DNA was isolated from the brain sample by using GenElute Mammalian Genomic DNA miniprep Kit (Sigma, #g1n70) and total 5-methylcytosin (5-mC) was determined using the 5-mC DNA ELISA Kit (Zymo Research Corp., #d5325) as per the manufacturer's instruction. The kit utilized an anti-5-methylcytosine monoclonal antibody that is both sensitive and specific for 5-mC. The result was expressed in percent 5-mC in a DNA sample calculated through a standard curve generated with specially designed controls included in the kit.

2.8. Real-time quantitative polymerase chain reaction analysis

Total RNA was isolated from brain tissue with Trizol ® Reagent (Thermo Fisher Scientific, USA). For RT-qPCR analysis, single-stranded cDNA was prepared from RNA by reverse transcription using oligo (dT) primers. Messenger RNA (mRNA) expression was quantified by the SYBR green-based qRT-PCR kit and specific oligo primers in a real-time quantitative PCR system (Stratagene Mx3000P, Agilent Technologies, Germany). After an initial denaturation step of 95 °C for 30 s, 40 cycles of PCR were performed. Each cycle consisted of a melting step at 95 °C for 15 s and an annealing an extension step at 60 °C for 1 min. The comparative Ct ($2^{-\Delta\Delta Ct}$) method was used to analyze the relative expression of mRNAs, which were normalized to *Gapdh*. The list of primers along with their sequences is shown in Table 1.

2.9. Gene-specific DNA methylation determination

Using the CpG island finder program (genome.ucsc.edu), we analyzed DNA methylation of one CpG island located at exon 1 of *Syn* and exon 2 of *Psd95*. The OneStep qMethyl™ kit was used for detecting gene-specific DNA methylation via selective amplification of methylated cytosines (5-mC) in the CpG island. Briefly, 20 ng of genomic DNA was incubated in the presence (test reaction) or absence (reference reaction) of methyl-sensitive restriction enzymes (5 U each) (AccII, HpyCH4IV and HpaII) at 37 °C for 2 h, followed by real-time PCR (RT-PCR). HpaII can be blocked by both 5-mC and 5hmC (hydroxymethylcytosine). However, 5hmC was ignored in this study because of its low content in the target sequences (129 bp-220 bp). After an initial denaturation step of 95 °C for 10 min, 45 cycles of PCR were performed. Each cycle consisted of a melting step at 95 °C for 30 s, an annealing step at 55 °C for 1 min and an extension step at 72 °C for 1 min. Final extension at 72 °C for 7 mins was performed prior to the hold step. Percentage methylation was calculated using the formula $100 \times 2^{-\Delta Ct}$, where ΔCt is the average Ct value from the test reaction minus the average Ct value from the reference

Table 1 List of the different primers used in the study.

Gene	Forward primers	Reverse primers	Accession No./Location
Syn	5′-CTGCTGGCAGACATGGACGT-3′	5′-AAAGGCGAAGATGGCAAAGAC-3′	NM_012664.3
Psd95	5′-GCAGGTTGCAGATCGGAGAC-3′	5′-CCAGGTGCTGAGAATATGAGGTT-3′	NM_019621.1
Dnmt1	5′-GAGTGGGATGGCTTCTTCAG-3′	5′-GTGTCTGTCCAGGATGTTG-3′	NM_053354.3
Dnmt3a	5′-ACGCCAAAGAAGTGTCTGCT-3′	5′-CTTTGCCCTGCTTTATGCAG-3′	XM_017594267.1
Dnmt3b	5′-TTCTCATGATGCCAAAGCTC-3′	5′-GAGGTTCTTTGCCTCTCCAG-3′	NM_001003959.1
Tet1	5′-GCAATCCGCAGAAAGCTTAG-3′	5′-TCACTCTCCACTCGCAGCTA-3′	XM_017601794.1
Tet2	5′-CCCAGGAAAGCACAGACATAG-3′	5′-AGCACCATTAGGCATTAGCAC-3′	XM_227694.8
Tet3	5′-TCAGCAACACCTTCATCACAA-3′	5′-TTTTCCTTGGGTGGTTTGTCA-3′	XM_008763094.2
Gapdh	5′-ACTCCCTCAAGATTGTCAGCA-3′	5′-CAGTCTTCTGAGTGGCAGTGAT-3′	XM_017592435.1
MGMT	5′-GGTGTGAAAACTTTGAAGGA-3′	5′-CACTATTCAAATTCCAACCC-3′	chr10: 129468335-129468531
Exon 1 of *Syn*	5′-CGACCGTGTCCCTGCTAC-3′	5′-CAGACATGGACGTGGTGAAT-3′	chrX: 15709106-15709235
Exon 2 of *Psd95*	5′-AGCTAGAGGCTCTGGACTGG-3′	5′-TACCTTGATGGGGGAGAGGT-3′	chr10: 56635972-56636192

reaction. Percentage methylation was relative to each experiment. To validate the accuracy of the OneStep qMethyl™ kit procedure for determining methylation percentage, the methylation level of the Human Methylated and Non-methylated DNA Standards was determined to be 95.8% and 6.2%, respectively, at the region spanned by the MGMT primers. The actual values were ˜97% and 6.0%, as determined by bisulfite sequencing methods. Primers were designed by using Primer3 (biotools.umassmed.edu) and their sequences are shown in Table 1.

2.10. Tissue collection

At 2 h after CPP test, rats were fully anesthetized with isoflurane, transcardially perfused with saline solution, then the VTA tissues were collected for Transmission electron microscopy ($n = 5$ per tissue). Proteins, total DNA and RNA were extracted from the same sample ($n = 6$ per tissue) for Western blotting, DNA methylation and mRNA expression.

2.11. Statistical analysis

Data were expressed as the mean ± standard error (S.E.M.). Preference in the drug-paired chamber and distance traveled were analyzed using two-way analysis of variance (ANOVA) with repeated measurements, with groups as between-subjects factors and days as within-subjects factors. Data were analyzed for significant differences using the Bonferroni test when appropriate.

Western blotting, RT-qPCR, and DNA methylation data were analyzed by one-way ANOVA performed with Bonferroni test. Bonferroni tests were only run if F achieved $p < 0.05$ and there was no significant variance inhomogeneity. All relevant *F*-values are provided in Supplementary file 1. Graphical presentation was performed using Graph Pad Prism 6.0 (Graph Pad Software, San Diego, CA, USA). Statistical analysis was performed using SPSS 13.0 software for Windows (SPSS Inc, Chicago, IL, USA). The level of significance was set at a p value of < 0.05.

3. Results

3.1. Oxytocin via its receptor blocked Oxy CPP

Firstly, the effect of OT on Oxy CPP was evaluated. It was shown that Oxy-treated rats spent a longer time in the drug-paired chamber, while no preference for either chamber was seen in the Sal+aCSF group (Fig. 2). This indicated that Oxy produced a significant place preference ($p < 0.05$) in rats. OT could significantly ($p < 0.05$) reduce preference in the Oxy-paired chamber compared with the Oxy+aCSF group. Ato markedly ($p < 0.05$) attenuated the inhibitory effect of OT on CPP. OT alone did not induce preference

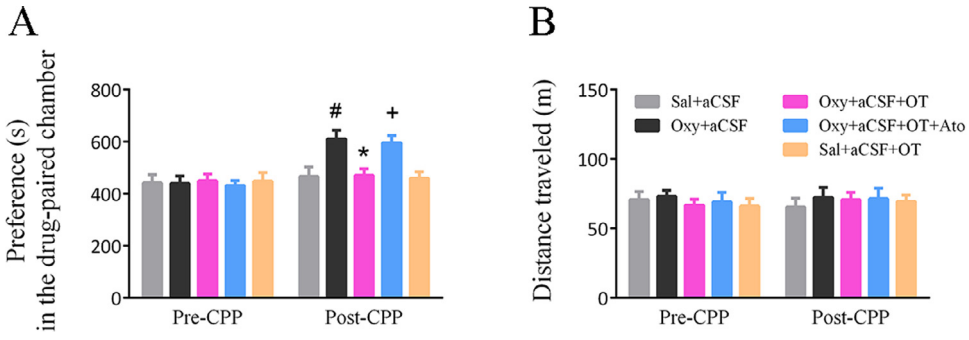

Fig. 2 OT - via its receptor - blocked Oxy CPP. The results are presented as the means ± S.E.M., two-way ANOVA with repeated measures, followed by Bonferroni test between each group within post-CPP, $^{\#}p < 0.05$ difference between preferences in the drug-paired chamber (A, $n = 11$/group) in the Oxy+aCSF group compared with the Sal+aCSF group, $^{*}p < 0.05$ indicates significant differences in the Oxy+ aCSF+OT group compared with the Oxy+aCSF group, $+p < 0.05$ indicates significant differences in the Oxy+aCSF+OT+Ato group compared with the Oxy+ aCSF+OT group. There were no differences for distance traveled (B, $n = 11$/group) in any of the groups.

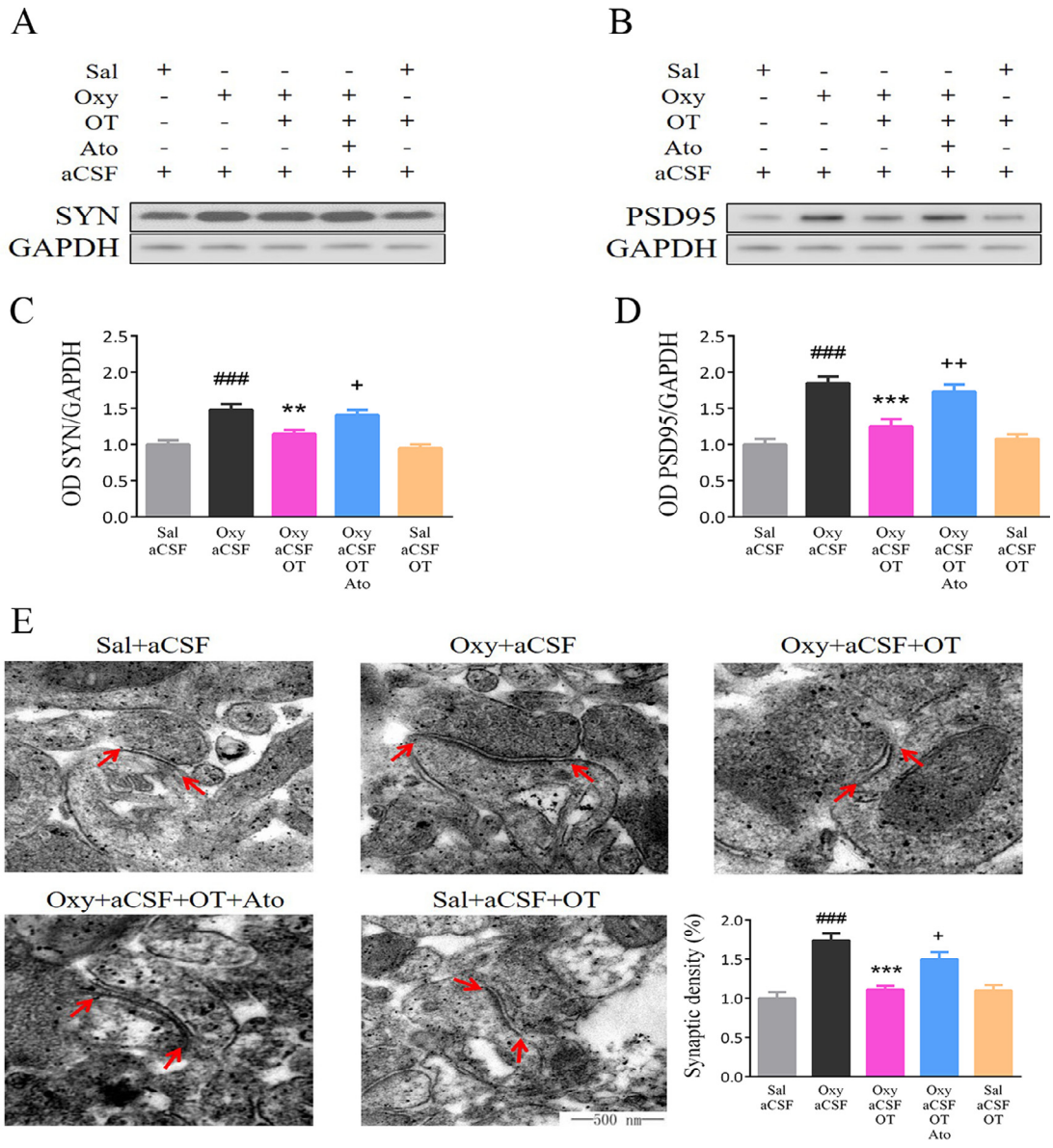

Fig. 3 OT reduced the expression of synaptic proteins and synaptic density in Oxy-treated rats. Representative (A, B) and quantitative (C, D) Western blot assays ($n = 6$/group) displaying the expression of SYN and PSD95 in the VTA. Representative and quantitative TEM images of synaptic density (E, marked by red arrows) in the different treatment groups ($n = 5$/group). Each brain sample was replicated three times in Western blot assays. One-way ANOVA followed by Bonferroni tests, $^{\#\#\#}p < 0.001$, compared with the Sal+aCSF group, $^{**}p < 0.01$, $^{***}p < 0.001$, compared with the Oxy+aCSF group, $^{+}p < 0.05$, $^{++}p < 0.01$ compared with the Oxy+aCSF+OT group.

in the drug-paired chamber compared with the Sal+aCSF group. For distance traveled (Fig. 2B), there were no differences between any of the groups. These results showed that OT - via its receptor - specifically prevented CPP induced by Oxy.

3.2. Oxytocin reduced the expression of synaptic proteins and synaptic density in Oxy-treated rats

The expression of synaptic proteins (SYN and PSD95) was evaluated after post-CPP. Western blot assays demonstrated that Oxy treatment significantly increased levels of SYN ($p < 0.001$) and PSD95 ($p < 0.001$) in the VTA (Fig. 3A-D). These changes were significantly attenuated by OT pretreatment (SYN: $p < 0.01$; PSD95: $p < 0.001$). Ato inhibited the effect of OT on Oxy-induced synaptic protein alteration (SYN: $p < 0.05$; PSD95: $p < 0.01$). Further morphological analysis in synaptic density was determined by TEM. The images showed that Oxy increased synaptic density compared with the Sal+aCSF group (Fig. 3E; $p < 0.001$). OT reduced synaptic density in Oxy-treated rats ($p < 0.001$) and Ato inhibited the effect of OT on synaptic density ($p < 0.05$). Following synapse detection, there were no significant differences

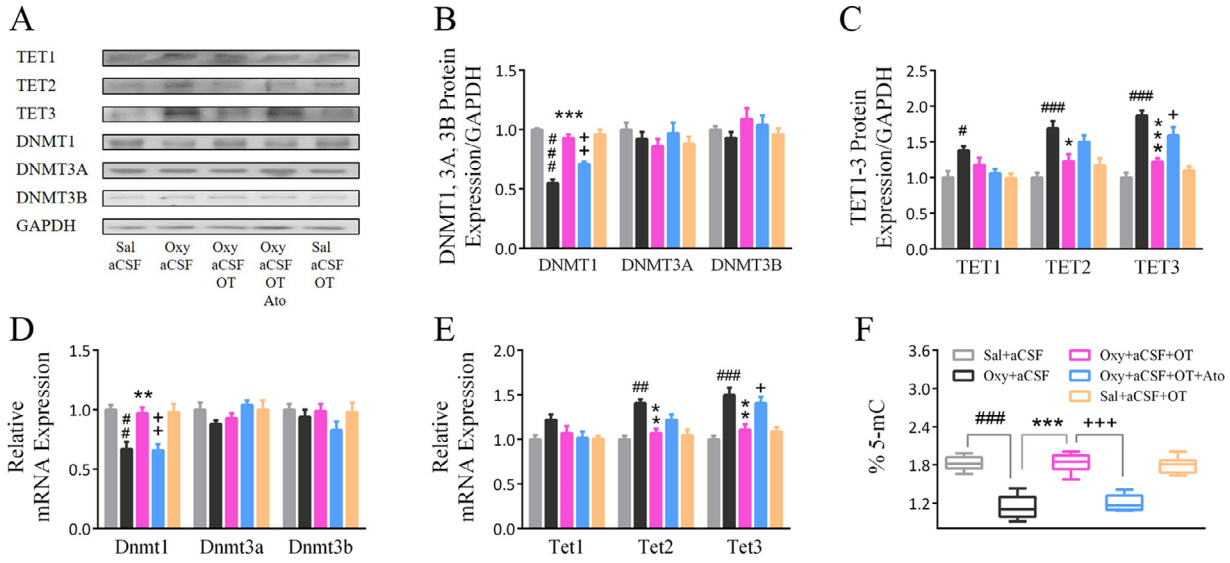

Fig. 4 OT differentially altered levels of DNMTs and TETs, and redistributed 5-mC in the VTA. Representative (A) and quantitative Western blot assays displaying the expression of DNMTs (B) and TETs (C). RT-qPCR assays displaying the transcription of DNMTs (D) and TETs (E) in the VTA. Levels of 5-mC (F) showing the global DNA methylation status. Each brain sample ($n = 6$/group) was replicated three times in Western blot assays. One-way ANOVA followed by Bonferroni tests, $^{\#}p < 0.05$, $^{\#\#}p < 0.01$, $^{\#\#\#}p < 0.001$, compared with the Sal+aCSF group, $^{*}p < 0.05$, $^{**}p < 0.01$, $^{***}p < 0.001$ compared with the Oxy+aCSF group, $^{+}p < 0.05$, $^{++}p < 0.01$, $^{+++}p < 0.001$ compared with the Oxy+aCSF+OT group.

between the Sal+aCSF+OT and Sal+aCSF groups. These results corroborate the Post-CPP test that OT - via its receptor - specifically reduced synaptic function in Oxy-treated rats.

3.3. Oxytocin differentially altered DNMTs and TETs level, and redistributed 5-mC in the VTA

In order to verify whether DNA methylation was involved in changing synaptic function, we investigated the expression of DNMT 1, 3A, 3B, and TET1-3 in the VTA. Oxy treatment caused a significant decrease in levels of DNMT1 ($p < 0.001$), and an increase in TET1 ($p < 0.05$), TET2 ($p < 0.001$), and TET3 ($p < 0.001$) relative to the Sal+aCSF group (Fig. 4A-C). Pretreatment with OT increased DNMT1 ($p < 0.001$) and decreased TET1, TET2 ($p < 0.05$), TET3 ($p < 0.001$) levels compared with the Oxy+aCSF group. Ato inhibited the effect of OT on Oxy-induced changes in the expression of DNMT1 ($p < 0.001$), TET2 and TET3 ($p < 0.05$). We also measured the mRNA expression of DNMTs and TETs in the VTA. Oxy treatment caused a significant decrease in DNMT1 ($p < 0.01$), and an increase in TET2 ($p < 0.01$), TET3 ($p < 0.001$) relative to the Sal+aCSF group (Fig. 4D, E). Pretreatment with OT increased DNMT1 ($p < 0.01$) and decreased TET2 ($p < 0.01$), and TET3 ($p < 0.01$) compared with the Oxy+aCSF group. Ato inhibited the effect of OT on Oxy-induced changes in DNMT1 ($p < 0.01$) and TET3 ($p < 0.05$). Alteration in levels of DNMTs and TETs induced by Oxy could be a result of changes in genomic DNA methylation associated with CpG islands. Accordingly, we found that Oxy treatment decreased 5-mC levels ($p < 0.001$), and pretreatment with OT significantly increased 5-mC ($p < 0.001$) levels in Oxy-treated rats; Ato completely blocked the effect of OT ($p < 0.001$). We did not find any differences in levels of DNMTs, TETs or 5-mC between the Sal+aCSF and Sal+aCSF+OT groups. These results indicated that OT - via its receptor - specifically regulated DNA methylation status in Oxy-treated rats.

3.4. Oxytocin increased DNA methylation at the exon 1 of *Syn* and exon 2 of *Psd95*

The expression of a particular gene may be up-regulated through a decrease in DNA methylation at CpG islands. Therefore, we explored Oxy-induced DNA methylation changes at the *Syn* and *Psd95* genes (Fig. 5A, B) and the effect of OT. We found that Oxy caused hypomethylation of exon 1 of *Syn* and exon 2 of *Psd95* (Fig. 5C, D; *Syn*: $p < 0.05$; *Psd95*: $p < 0.01$), followed by an increase in the expression of SYN and PSD95 mRNA (Fig. 5E, F; SYN: $p < 0.05$; PSD95: $p < 0.01$) compared with the Sal+aCSF group. Pretreatment with OT (prior to Oxy treatment) increased methylation of exon 1 of *Syn* and exon 2 of *Psd95* ($p < 0.05$), and decreased SYN and PSD95 mRNA expression ($p < 0.05$) in Oxy-treated rats. Ato inhibited the effect of OT on Oxy-induced CpG island hypomethylation at exon 1 of *Syn* and exon 2 of *Psd95* ($p < 0.05$), restoring the increase in mRNA expression of SYN and PSD95 ($p < 0.05$). OT alone did not affect DNA methylation or mRNA expression compared with the Sal+aCSF group. These results suggest that OT - via its receptor - specifically inhibited the Oxy-induced increase in SYN and PSD95 mRNA by increasing methylation of *Syn* and *Psd95*.

4. Discussion

In this study, we have made three main findings: (1) DNA hypomethylation at the exons of *Syn* and *Psd95* contributed to Oxy CPP. (2) OT - via its receptor - blocked Oxy-induced DNA

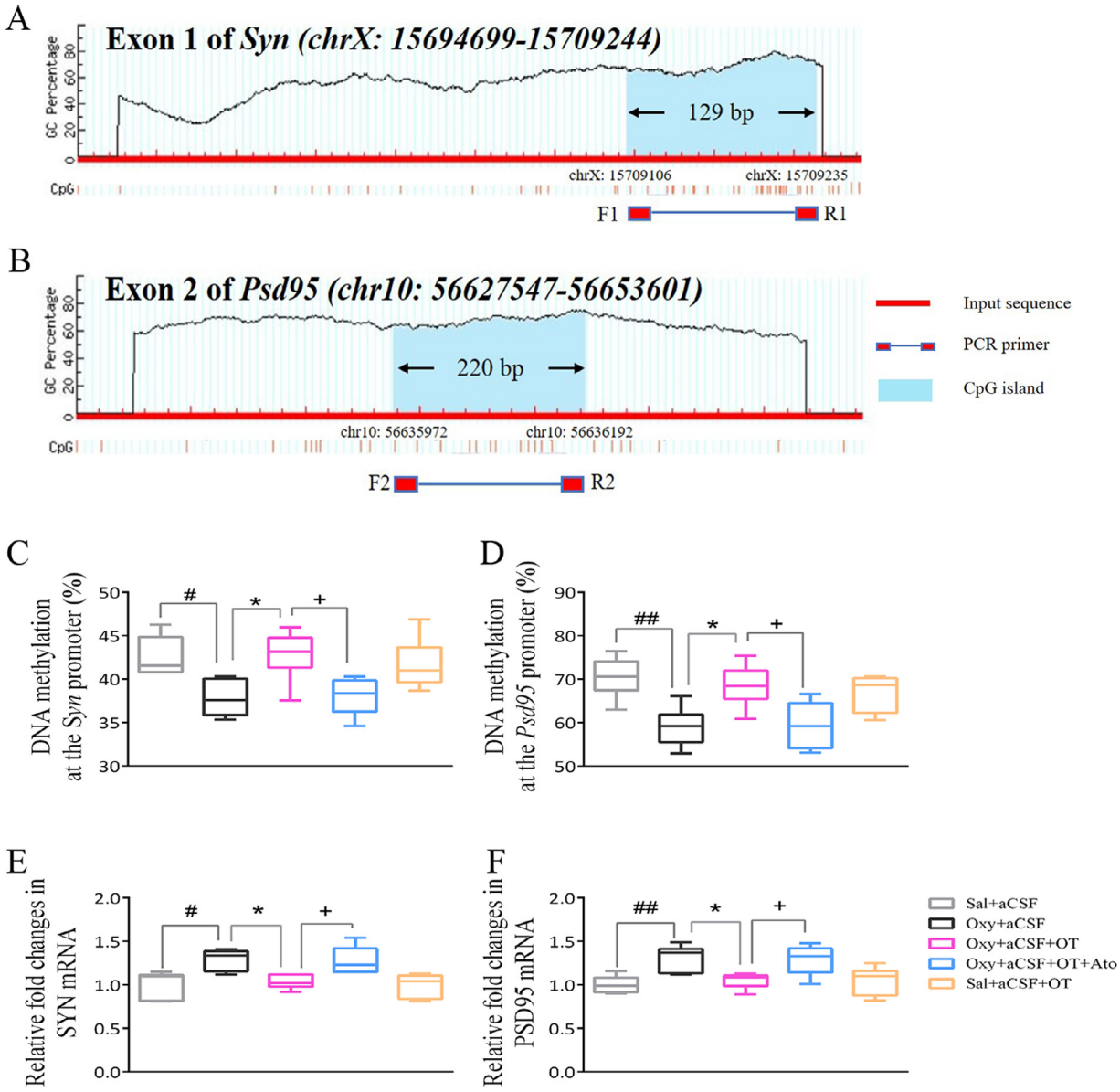

Fig. 5 OT increased DNA methylation at exon 1 of *Syn* and exon 2 of *Psd95*. Bioinformatics analysis of the CpG islands at the *Syn* (A) and *Psd95* (B) genes. The CpG islands indicated the locations of primer pairs for DNA methylation detection. OT pretreatment elevated methylation of exon of *Syn* (C, $n = 6$/group) and *Psd95* (D, $n = 6$/group) in Oxy-treated rats. The effect of OT on Oxy-induced changes in SYN (E, $n = 6$/group) and PSD95 (F, $n = 6$/group) mRNA. One-way ANOVA followed by Bonferroni tests, $^{\#}p < 0.05$, $^{\#\#}p < 0.01$ compared with the Sal+aCSF group, $^{*}p < 0.05$ compared with the Oxy+aCSF group, $^{+}p < 0.05$ compared with the Oxy+aCSF+OT group.

hypomethylation of *Syn* and *Psd95* in the VTA. (3) OT specifically recovered the synaptic function in Oxy-treated rats and inhibited the CPP acquisition induced by Oxy. Therefore, OT could be a potential new candidate for treating Oxy addiction.

Environmental stimuli (cues) that are repeatedly associated with a drug are known to promote compulsive drug taking and are a primary trigger of relapse (See, 2002). Here, we examined whether a stationary-dose (3.0 mg/kg), one-binge regimen of Oxy administered to rats within 8 days induced CPP. We found that rats spent a significantly longer time in the drug-paired chamber after Oxy treatment compared with untreated rats (Fig. 2A). This indicated that cues in the CPP chamber were sufficient to elicit abnormal learning and memory consolidation on Oxy craving. Our studies were consistent with those reporting that rats repeatedly exposed to Oxy showed CPP (Iriah et al., 2019; Ryan et al., 2018). The neural circuits that are involved in developing addictive behaviors and that are responsive to neurotransmitters, namely, the nucleus accumbens, amygdala, prefrontal cortex and VTA are also responsible for consolidation of drug-associated memories (Taylor et al., 2009). Evidence has shown that Oxy enhanced rewarding effects, mainly due to the excessive release of dopamine or abnormal activation of the dopamine receptor 1 in the VTA (Sanchez et al., 2016). The adaptive changes in the

brain may include alterations in structural modifications at synapses (Robison and Nestler, 2011). A single injection of morphine or heroin has been reported to up-regulate the expression of c-Fos, JunB and Egri in rats (Liu et al., 1994; Rawas et al., 2009). In this investigation, the effects of Oxy on a family of proteins that have been shown to play an important role in synaptic plasticity were evaluated, namely SYN and PSD95. SYN is located in presynaptic terminals (Greengard et al., 1993) and promotes synaptogenesis, and regulates vesicle dynamics and neurotransmitter release (Fornasiero et al., 2010). Indeed, given the consistency of the effects caused by Oxy on SYN expression (Fig. 3C), it is very likely that this protein could be an important node that connects various networks involved in the early manifestations, maintenance of, and - possibly - relapse of addiction. PSD95 is specifically associated with the postsynaptic membrane density at excitatory synapses (Hunt et al., 1996) and, therefore, provides only a selective indication of postsynaptic preservation or loss. Indeed, we found that changes in synaptic density (Fig. 3E) induced by Oxy was associated with PSD95 protein (Fig. 3D). Thus, our observations of Oxy-induced changes in the expression of these synaptic proteins could be relevant to the report showing that exposure to opiates caused changes in the density of dendritic spines, changes that were dependent on activation of the RhoA pathway (Cahill et al., 2018). Our finding that Oxy increased SYN and PSD95 proteins (Fig. 3C, D), suggests that the drug could enhance the functionality of synapses in rats.

DNA methylation causes stable epigenetic marks that may translate environmental changes into transcriptional regulation. The DNA methylation machinery, including DNMTs and TETs, is dysregulated in brain reward pathways after drug exposure (Vaillancourt et al., 2017; Saad et al., 2019). When comparing DNMT expression in response to Oxy, the most prominent difference was observed for DNMT1 (Fig. 4B). In line with our study, Jayanthi and colleagues (Jayanthi et al., 2014) reported that chronic methamphetamine exposure changed the expression of DNMT1, but not DNMT3A or DNMT3B (Jayanthi et al., 2014). DNMT1 is essential for maintaining DNA methylation patterns, while DNMT3A and DNMT3B are also required for de novo methylation (Siedlecki and Zielenkiewicz, 2006); it is noteworthy that these enzymes have overlapping and different target genes and functions (Challen et al., 2014). Consistent with these studies, DNMTs were found to be modulated by repeated drug exposure with a daily biphasic expression (LaPlant et al., 2010; Anier et al., 2010). Here, we only reported the changes in expression of DNMTs at 2 h after post-CPP. The role of DNMT3A and DNMT3B in Oxy-induced CPP cannot be completely excluded from regulation by Oxy. Thus, further studies need to be carried out to investigate dynamic changes in DNMTs following Oxy CPP. Similar to DNMTs, TET proteins recognize common and specific 5-mC target sequences (Rasmussen and Helin, 2016). Since these proteins are activated by Oxy, less 5-mC should be generated in the VTA (Fig. 4). Hence, changes in the relative levels of DNA methylation may lead to altered gene expression. We therefore hypothesize that there is a CpG island which is modified on the *Syn* and *Psd95* genes. In order to test the idea that Oxy-induced gene expression could be regulated by epigenetic modifications, we demonstrated that Oxy resulted in decreased methylation at exon 1 of *Syn* and exon 2 of *Psd95* (Fig. 5C, D). It was also found that the exons of *Syn* and *Psd95* hypomethylation corresponded with increased expression of SYN and PSD95 mRNA (Fig. 5E, F). Taken together with other available data, our results demonstrate that DNMT1 and TET1-3 represent the major enzymes differentially regulated by Oxy. Our findings also indicate that the *Syn* and *Psd95* genes are regulated at an epigenetic level and that they may work together to maintain Oxy-induced CPP. In addition to *Syn* and *Psd95* genes, previous studies have shown that DNA methylation at specific regulatory sites in the OT receptor gene is associated with mental disorders (Lancaster et al., 2018; Perkeybile et al., 2019; Ebner et al., 2019). In the present study, we did not explore whether OT receptor gene methylation was regulated by Oxy. In order to fully understand the mechanism of Oxy CPP, further investigations of OT receptor gene methylation should be carried out.

OT receptors are G-protein-coupled receptors (GPCRs) comprising different subunits (Gq, Gi1, Gi2, Gi3, GoA and GoB; Busnelli and Chini, 2017). Ato (the selective antagonist of OT receptor) activates different signaling pathway by coupling with different types of G protein (Manning et al., 2008; Reversi et al., 2005; Busnelli et al., 2012; Chini and Manning, 2007), suggesting that Ato alone could have an effect on behavioral and biomolecular responses. Indeed, γ-aminobutyric acid (GABA) levels were significantly increased in the hypothalamus and midbrain after 30 days of exposure to Ato (Thakur et al., 2019). However, short-term injection of Ato did not affect spatial memory (Salighedar et al., 2019), locomotive activity or methamphetamine-induced CPP (Qi et al., 2009) in rodents. It has also been reported that Ato administration alone had no effect on the firing of dopamine neurons in the VTA (Leng et al., 2019) or on dopamine metabolism in the striatum (Qi et al., 2008). These studies indicated that Ato activates different behavioral or molecular responses in the CNS according to the time period of drug administration. In the present study, the time point of Ato administration we chose was in accordance with the study by Qi and colleagues.

Many studies have demonstrated that OT specifically inhibits the acquisition of CPP, facilitates the extinction of drug-induced CPP and abolishes the reinstatement of CPP induced by restraint stress; these effects of OT can be attenuated by Ato (Qi et al., 2009); The OT analogue carbetocin prevents priming/emotional impairment/stress-induced reinstatement of opioid seeking (Georgiou et al., 2015b; Zanos et al., 2014b). These investigations suggest that OT - via its receptor - plays an important regulatory role in drug addiction. Therefore, our efforts to develop effective treatments for Oxy craving have focused on manipulations of CPP processes involved in encoding cue-drug associations. At the behavioral levels, we found that OT - via its receptor - markedly delayed CPP induced by Oxy (Fig. 2A). Given that Oxy stimulation causes changes in synaptic function (Fig. 3C–E), activation of the OT receptor and reduction of synaptic density in Oxy-treated rats indicate a protective effect of OT. This is the first study to show that OT could reshape synaptic structures via its receptor. In a similar study, it was reported that intranasal administration of OT was effective in inhibiting stress-induced alterations in hippocampal plasticity (Lee et al., 2015); OT

- via its receptor - was also shown to inhibit drug-induced changes in glutamate receptor (NR1) and transporter (GLT1) expression (Qi et al., 2012). Here, we also demonstrated that epigenetic modifications could be an important mechanism in the inhibitory effect of OT on Oxy CPP. We have shown, for the first time, that OT - via its receptor - activated DNMT1 and repressed TET2-3 (Fig. 4B, C), and also blocked hypomethylation at the exons of *Syn* and *Psd95* (Fig. 5D) in Oxy-treated rats. DNMT1 and TET2-3 are likely to be the main target sites that are affected by OT. However, we were unable to determine which TET subtype was important for OT action. It is possible that TET2 and TET3 worked together to hypermethylate the CpG islands, followed by transcriptional repression of these genes.

The neural mechanisms of OT administration underlying drug addiction are intricate, including neurotransmitter or hormone release (Estes et al., 2019; Flanagan et al., 2019), GABAergic interneuron firing (Diaz et al., 2011), as well as Fos expression (Kohtz et al., 2018). However, OT and DNA methylation is thought to interact, leading to inhibition of drug-induced changes in learning and memory (Fan et al., 2018). Fan and colleagues demonstrated that OT pretreatment inhibited methamphetamine-induced decreases in DNMT1, DNMT3A, DNMT3B and MECP2 in the hippocampus, blocked DNA methylation changes at the *Syn* promoter, and finally attenuated spatial memory in methamphetamine-treated mice. Their findings contribute to growing evidence suggesting that OT pretreatment regulating DNA methylation at specific sites of synaptic genes are associated with the inhibition of abnormal learning and memory-induced drug addiction.

5. Conclusions

Our results have demonstrated that DNA hypomethylation at the exons of *Syn* and *Psd95* in the VTA play a crucial role in Oxy CPP, likely mediated by inhibition of DNMT1 and activation of TET1-3. OT - via its receptor - specifically inhibited the establishment of CPP by DNA re-methylation at the exons of *Syn* and *Psd95*, mediated by stimulating DNMT1 and TET2-3. We suggest that the function of OT in reversing DNA methylation could have a potential therapeutic effect for treating oxycodone addiction.

Declaration of transparency and scientific rigor

This declaration acknowledges that this paper adheres to the principles for transparent reporting and scientific rigor of preclinical research recommended by funding agencies, publishers and other organizations engaged with supporting research.

Role of the funding source

National Nature Science Foundation of China; the Key Research and Development Program of Liaoning Province; the Outstanding Scientific Fund of Shengjing Hospital.

Contributors

X.-Y. F. designed the study and wrote the manuscript. G. S. analyzed data and revised the manuscript. X.-Y. F. and G. S. performed the research. P. Z. supervised the study.

Conflict of interest

The authors declare no conflict of interest.

Acknowledgments

We are grateful to Yong-Da Liu and Zi-Yi Wu for assisting during behavioral study. We also thank Gui-Feng Zhao for feeding the rats and the support from the staff. This work was supported by the National Natural Science Foundation of China (Nos. 81671311 and 81870838), the Key Research and Development Program of Liaoning Province (No. 2018225004), and the Outstanding Scientific Fund of Shengjing Hospital (No. 201708).

Supplementary materials

Supplementary material associated with this article can be found, in the online version, at doi:10.1016/j.euroneuro.2019.10.010.

References

Amini-Khoei, H., Amiri, S., Mohammadi-Asl, A., Alijanpour, S., Poursaman, S., Haj-Mirzaian, A., et al., 2017. Experiencing neonatal maternal separation increased pain sensitivity in adult male mice: involvement of oxytocinergic system. Neuropeptides 61, 77–85.

Anier, K., Malinovskaja, K., Aonurm-Helm, A., Zharkovsky, A., Kalda, A., 2010. Dna methylation regulates cocaine-induced behavioral sensitization in mice. Neuropsychopharmacology 35 (12), 2450–2461.

Baracz, S.J., Parker, L.M., Suraev, A.S., Everett, N.A., Goodchild, A.K., Mcgregor, I.S., et al., 2016. Chronic methamphetamine self-administration dysregulates oxytocin plasma levels and oxytocin receptor fibre density in the nucleus accumbens core and subthalamic nucleus of the rat. J. Neuroendocrinol. 28 (4). doi:10.1111/jne.12337.

Befort, K., Filliol, D., Ghate, A., Darcq, E., Matifas, A., Muller, J., et al., 2010. Mu-opioid receptor activation induces transcriptional plasticity in the central extended amygdala. Eur. J. Neurosci. 27 (11), 2973–2984.

Bian, E.B., Zong, G., Xie, Y.S., Meng, X.M., Huang, C., Li, J., et al., 2014. Tet family proteins: new players in gliomas. J. Neurooncol. 116 (3), 429–435.

Boccia, M.M., Kopf, S.R., Baratti, C.M., 1998. Effects of a single administration of oxytocin or vasopressin and their interactions with two selective receptor antagonists on memory storage in mice. Neurobiol. Learn. Mem. 69, 136–146.

Busnelli, M., Saulière, A., Manning, M., Bouvier, M., Galés, C., Chini, B., 2012. Functional selective oxytocin-derived agonists discriminate between individual g protein family subtypes. J. Biol. Chem. 287 (6), 3617–3629.

Busnelli, M., Chini, B., 2017. Molecular basis of oxytocin receptor signalling in the brain: what we know and what we need to know. Curr. Top. Behav. Neurosci 35, 3–29.

Cahill, M.E., Browne, C.J., Wang, J., Hamilton, P.J., Dong, Y., Nestler, E.J., 2018. Withdrawal from repeated morphine admin-

istration augments expression of the RhoA network in the nucleus accumbens to control synaptic structure. J. Neurochem. 147 (1), 84–98.
Challen, G., Sun, D., Mayle, A., Jeong, M., Luo, M., Rodriguez, B., et al., 2014. Dnmt3a and dnmt3b have overlapping and distinct functions in hematopoietic stem cells. Cell Stem Cell 15 (3), 350–364.
Chini, B., Manning, M., 2007. Agonist selectivity in the oxytocin/vasopressin receptor family: new insights and challenges. Biochem. Soc. Trans. 35 (4), 737–741.
Colonnier, M., Beaulieu, C., 1985. An empirical assessment of stereological formulae applied to the counting of synaptic disks in the cerebral cortex. J. Comp. Neurol. 231, 175–179.
Cox, B.M., Bentzley, B.S., Regentuero, H., See, R.E., Reichel, C.M., Astonjones, G., 2016. Oxytocin acts in nucleus accumbens to attenuate methamphetamine seeking and demand. Biol. Psychiatry 81 (11), S0006322316330554.
De Oliveira, L.F., Camboim, C., Diehl, F., Consiglio, A.R., Quillfeldt, J.A., 2007. Glucocorticoid-mediated effects of systemic oxytocin upon memory retrieval. Neurobiol. Learn. Mem. 87, 67–71.
Diaz, M.R., Chappell, A.M., Christian, D.T., Anderson, N.J., McCool, B.A., 2011. Dopamine D3-like receptors modulate anxiety-like behavior and regulate GABAergic transmissionin the rat lateral/basolateral amygdala. Neuropsychopharmacology 36 (5), 1090–1103.
DeFelipe, J., Marco, P., Busturia, I., Merchan-Perez, A., 1999. Estimation of the number of synapses in the cerebral cortex: methodological considerations. Cereb. Cortex 9, 722–732.
Detich, N., Hamm, S., Just, G., Knox, J.D., Szyf, M., 2003. The methyl donor S-adenosylmethionine inhibits active demethylation of DNA. J. Biol. Chem. 278 (23), 20812–20820.
Dobs, Y.E., Ali, M.M., 2019. The epigenetic modulation of alcohol/ethanol and cannabis exposure/co-exposure during different stages. Open Biol. 9 (1), 180115.
Ebner, N.C., Lin, T., Muradoglu, M., Weir, DH., Plasencia, G.M., Lillard, T.S., et al., 2019. Associations between oxytocin receptor gene (OXTR) methylation, plasma oxytocin, and attachment across adulthood. Int. J. Psychophysiol. 136, 22–32.
Estes, M.K., Freels, T.G., Prater, W.T., Lester, D.B., 2019. Systemic oxytocin administration alters mesolimbic dopamine release in mice. Neuroscience 408, 226–238.
Everett, N.A., Mcgregor, I.S., Baracz, S.J., Cornish, J.L., 2018. The role of the vasopressin v1a receptor in oxytocin modulation of methamphetamine primed reinstatement. Neuropharmacology 133, 1–11.
Fan, X.Y., Yang, J.Y., Dong, Y.X., Hou, Y., Liu, S., Wu, C.F., 2018. Oxytocin inhibits methamphetamine-associated learning and memory alterations by regulating DNA methylation at the Synaptophysin promoter. Addict. Biol. doi:10.1111/adb.12697.
Fiona, L., Stefano, G., Francesca, B., Busceti, C.L., Francesco, F., 2018. Epigenetic effects induced by methamphetamine and methamphetamine-dependent oxidative stress. Oxid. Med. Cell Longev. 2018, 1–28.
Flanagan, J.C., Allan, N.P., Calhoun, C.D., Badour, C.L., Moran-Santa, Maria, M., Brady, K.T., et al., 2019. Effects of oxytocin on stress reactivity and craving in veterans with co-occurring PTSD and alcohol use disorder. Exp. Clin. Psychopharmacol. 27 (1), 45–54.
Fornasiero, E.F., Bonanomi, D., Benfenati, F., Valtorta, F., 2010. The role of synapsins in neuronal development. Cell. Mol. life Sci. 67, 1383–1396.
Georgiou, P., Zanos, P., Ehteramyan, M., Hourani, S., Kitchen, I., Maldonado, R., et al., 2015a. Differential regulation of mGlu5 R and MOPr by priming- and cue-induced reinstatement of cocaine-seeking behaviour in mice. Addict Biol 20 (5), 902–912.
Georgiou, P., Zanos, P., Garcia-Carmona, J.A., Hourani, S., Kitchen, I., Kieffer, B.L., et al., 2015b. The oxytocin analogue carbetocin prevents priming-induced reinstatement of morphine-seeking: involvement of dopaminergic, noradrenergic and MOPr systems. Eur. Neuropsychopharmacol. J. Eur. Coll. Neuropsychopharmacol. 25 (12), 2459–2464.
Georgiou, P., Zanos, P., Hourani, S., Kitchen, I., Bailey, A., 2016. Cocaine abstinence induces emotional impairment and brain region-specific upregulation of the oxytocin receptor binding. Eur. J. Neurosci. 44 (7), 2446–2454.
Georgiou, P., Zanos, P., Garcia-Carmona, J.A., Hourani, S., Kitchen, I., Laorden, M.L., et al., 2017. Methamphetamine abstinence induces changes in μ-opioid receptor, oxytocin and CRF systems: association with an anxiogenic phenotype. Neuropharmacology 105, 520–532.
Greengard, P., Valtorta, F., Czernik, A.J., Benfenati, F., 1993. Synaptic vesicle phosphoproteins and regulation of synaptic function. Sciencen 259, 780–785.
Hao, Y., Yang, J.Y., Sun, J.Y., Qi, J., Dong, Y.X., Wu, C.F., 2008. Lesions of the medial prefrontal cortex prevent the acquisition but not reinstatement of morphine-induced conditioned place preference in mice. Neurosci. Lett. 433, 48–53.
Hunt, C.A., Schenker, L.J., Kennedy, M.B., 1996. PSD-95 is associated with the postsynaptic density and not with the presynaptic membrane at forebrain synapses. J. Neurosci. 16, 1380–1388.
Iriah, S.C., Trivedi, M., Kenkel, W., Grant, S.E., Moore, K., Yee, J.R., et al., 2019. Oxycodone exposure: a magnetic resonance imaging study in response to acute and chronic oxycodone treatment in rats. Neuroscience 398, 88–101.
Jayanthi, S., Mccoy, M.T., Chen, B., Britt, J.P., Kourrich, S., Yau, H.J., et al., 2014. Methamphetamine downregulates striatal glutamate receptors via diverse epigenetic mechanisms. Biol. Psychiatry 76 (1), 47–56.
Kohtz, A.S., Lin, B., Smith, M.E., Aston-Jones, G., 2018. Attenuated cocaine-seeking after oxytocin administration in male and female rats. Psychopharmacology 235, 1–13.
Lancaster, K., Goldbeck, L., Puglia, M.H., Morris, J.P., Connelly, J.J., 2018. DNA methylation of OXTR is associated with parasympathetic nervous system activity and amygdala morphology. Soc. Cogn. Affect. Neurosci. 13 (11), 1155–1162.
Langlois, L.D., Dacher, M., Nugent, F.S., 2018. Dopamine receptor activation is required for GABAergic spike timing-dependent plasticity in response to complex spike pairing in the ventral tegmental area. Front. Synaptic Neurosci. 10, 32.
Langlois, L.D., Nugent, F.S., 2017. Opiates and plasticity in the ventral tegmental area. ACS Chem. Neurosci. 8 (9), 1830–1838.
Laplant, Q., Vialou, V., Covington, H.E., Dumitriu, D., Feng, J., Warren, B.L., et al., 2010. Dnmt3a regulates emotional behavior and spine plasticity in the nucleus accumbens. Nat. Neurosci. 13 (9), 1137–1143.
Lax, E., Warhaftig, G., Ohana, D., Maayan, R., Delayahu, Y., Roska, P., et al., 2018. A DNA methylation signature of addiction in T cells and its reversal with DHEA intervention. Front. Mol. Neurosci. 11, 322.
Lee, S.Y., Park, S.H., Chung, C., Kim, J.J., Choi, S.Y., Han, J.S., 2015. Oxytocin protects hippocampal memory and plasticity from uncontrollable stress. Sci. Rep. 5, 18540.
Leng, H., Zhang, X., Wang, Q., Luan, X., Sun, X., Guo, F., Gao, S., Liu, X., Xu, L., 2019. Regulation of stress-induced gastric ulcers via central oxytocin and a potential mechanism through the VTA-NAc dopamine pathway. Neurogastroenterol. Motil. 31 (9), e13655.
Liu, J., Nickolenko, J., Sharp, F.R., 1994. Morphine induces c-fos and jun b in striatum and nucleus accumbens via D1 and N-methyl-D-aspartate receptors. Proc. Natl. Acad. Sci. U.S.A. 91 (18), 8537–8541.
Liu, L., Zhu, J., Zhou, L., Wan, L., 2016. Rack1 promotes maintenance of morphine-associated memory via activation of an

ERK-CREB dependent pathway in hippocampus. Sci. Rep. 6 (1), 20183.
Maldonado, C., Rodriguez-Arias, M., Castillo, A., Aguilar, M.A., Minarro, J., 2007. Effect of memantine and CNQX in the acquisition, expression and reinstatement of cocaine-induced conditioned place preference. Progr. Neuro-Psychopharmacol. Biol. Psychiatry 31, 932–939.
Manning, M., Stoev, S., Chini, B., Durroux, T., Mouillac, B., Guillon, G., 2008. Peptide and non-peptide agonists and antagonists for the vasopressin and oxytocin v1a, v1b, v2 and OT receptors: research tools and potential therapeutic agents. Prog. Brain Res. 170, 473–512.
Marie-Claire, C., Crettol, S., Cagnard, N., Bloch, V., Mouly, Stéphane, Laplanche, J.L., et al., 2016. Variability of response to methadone: genome-wide dna methylation analysis in two independent cohorts. Epigenomics 8 (2), 181–195.
Mcrae-Clark, A.L., Baker, N.L., Maria, M.M., Brady, K.T., 2013. Effect of oxytocin on craving and stress response in marijuana-dependent individuals: a pilot study. Psychopharmacology 228 (4), 623–631.
Paxinos, G., Watson, C., 2013. The Rat Brain in Stereotaxic Coordinates, 7th ed, p. 388.
Perkeybile, A.M., Carter, C.S., Wroblewski, K.L., Puglia, M.H., Kenkel, W.M., Lillard, T.S., Karaoli, T., et al., 2019. Early nurture epigenetically tunes the oxytocin receptor. Psychoneuroendocrinology 99, 128–136.
Poetsch, A.R., Plass, C., 2011. Transcriptional regulation by dna methylation. Cancer Treat. Rev. 37 (Supp-S1), S8–S12. doi:10.1016/j.ctrv.2011.04.010.
Qi, J., Yang, J.Y., Song, M., Li, Y., Wang, F., Wu, C.F., 2008. Inhibition by oxytocin of methamphetamine-induced hyperactivity related to dopamine turnover in the mesolimbic region in mice. Naunyn Schmiedebergs Arch. Pharmacol. 376 (6), 441–448.
Qi, J., Yang, J.Y., Wang, F., Zhao, Y.N., Song, M., Wu, C.F., 2009. Effects of oxytocin on methamphetamine-induced conditioned place preference and the possible role of glutamatergic neurotransmission in the medial prefrontal cortex of mice in reinstatement. Neuropharmacology 56, 856–865.
Qi, J., Han, W.Y., Yang, J.Y., Wang, L.H., Dong, Y.X., Wang, F., et al., 2012. Oxytocin regulates changes of extracellular glutamate and GABA levels induced by methamphetamine in the mouse brain. Addict. Biol. 17, 758–769.
Rawas, R.E., Thiriet, N., Lardeux, V., Jaber, M., Solinas, M., 2009. Environmental enrichment decreases the rewarding but not the activating effects of heroin. Psychopharmacology 203 (3), 561–570.
Rasmussen, K.D., Helin, K., 2016. Role of TET enzymes in DNA methylation, development, and cancer. Genes. Dev. 30 (7), 733–750.
Remillard, D., Kaye, A.D., Mcanally, H., 2019. Oxycodone's unparalleled addictive potential: is it time for a moratorium? Curr. Pain Headache Rep. 23, 15.
Reversi, A., Rimoldi, V., Marrocco, T., Cassoni, P., Bussolati, G., Parenti, M., Chini, B., 2005. The oxytocin receptor antagonist atosiban inhibits cell growth via a "biased agonist" mechanism. J. Biol. Chem. 280 (16), 16311–16318.
Robison, A.J., Nestler, E.J., 2011. Transcriptional and epigenetic mechanisms of addiction. Nat. Rev. Neurosci. 12, 623–637.
Ryan, J.D., Zhou, Y., Contoreggi, N.H., Bshesh, F.K., Gray, J.D., Kogan, J.F., et al., 2018. Sex differences in the rat hippocampal opioid system after oxycodone conditioned place preference. Neuroscience 393, 236–257.
Saad, L., Sartori, M., Pol Bodetto, S., Romieu, P., Kalsbeek, A., Zwiller, J., et al., 2019. Regulation of brain DNA methylation factors and of the orexinergic system by cocaine and food self-administration. Mol. Neurobiol. doi:10.1007/s12035-018-1453-6.
Salighedar, R., Erfanparast, A., Tamaddonfard, E., Soltanalinejad, F., 2019. Medial prefrontal cortex oxytocin-opioid receptors interaction in spatial memory processing in rats. Physiol. Behav. 209, 112599.
Sanchez, V., Carpenter, M.D., Yohn, N.L., Blendy, J.A., 2016. Long-lasting effects of adolescent oxycodone exposure on reward-related behavior and gene expression in mice. Psychopharmacology. 233, 3991–4002.
Schuster, R., Kleimann, A., Rehme, M.K., Taschner, L., Glahn, A., Groh, A., et al., 2016. Elevated methylation and decreased serum concentrations of bdnf in patients in levomethadone compared to diamorphine maintenance treatment. Eur. Arch. Psychiatry Clin. Neurosci. 267 (1), 1–8.
See, R.E., 2002. Neural substrates of conditioned-cued relapse to drug-seeking behavior. Pharmacol. Biochem. Behav. 71, 517–529.
Siedlecki, P., Zielenkiewicz, P., 2006. Mammalian DNA methyltransferases. Acta Biochim. Pol. 53, 245 English Edition.
Singh, F., Nunag, J., Muldoon, G., Cadenhead, K.S., Pineda, J.A., Feifel, D., 2016. Effects of intranasal oxytocin on neural processing within a socially relevant neural circuit. Eur. Neuropsychopharmacol. 26 (3), 626–630.
Smaga, I., Sanak, M., Filip, M., 2019. Cocaine-induced changes in the expression of NMDA receptor subunits. Curr. Neuropharmacol. 17 (11), 1039–1055.
Sorg, B.A., 2012. Reconsolidation of drug memories. Neurosci. Biobehav. Rev. 36 (5), 1400–1417.
Stauffer, C.S., Moschetto, J.M., McKernan, S.M., Hsiang, E., Borsari, B., Woolley, J.D., 2019. Oxytocin-enhanced motivational interviewing group therapy for methamphetamine use disorder in men who have sex with men: study protocol for a randomized controlled trial. Trials 20, 145.
Sun, L., Zhao, J.Y., Gu, X., Liang, L., Wu, S., Mo, K., et al., 2017. Nerve injury-induced epigenetic silencing of opioid receptors controlled by dnmt3a in primary afferent neurons. Pain 158 (6), 1153–1165.
Taylor, J.R., Olausson, P., Quinn, J.J., Torregrossa, M.M., 2009. Targeting extinction and reconsolidation mechanisms to combat the impact of drug cues on addiction. Neuropharmacology 56, 186–195.
Thakur, P., Shrivastava, R., Shrivastava, V.K., 2019. Effects of exogenous oxytocin and atosiban antagonist on GABA in different region of brain. IBRO Rep. 6, 185–189.
Vaillancourt, K., Ernst, C., Mash, D., Turecki, G., 2017. DNA methylation dynamics and cocaine in the brain: progress and prospects. Genes 8, 138.
van Steenbergen, H., Eikemo, M., Leknes, S., 2019. The role of the opioid system in decision making and cognitive control: a review. Cogn. Affect. Behav. Neurosci. doi:10.3758/s13415-019-00710-6.
Wu, Q., Wei, G., Ji, F., Jia, S., Wu, S., Guo, X., et al., 2018. Tet1 overexpression mitigates neuropathic pain through rescuing the expression of μ-opioid receptor and kv1.2 in the primary sensory neurons. Neurotherapeutics 16 (2), 491–504.
Zanos, P., Wright, S.R., Georgiou, P., Ji, H.Y., Ledent, C., Hourani, S.M., et al., 2014a. Chronic methamphetamine treatment induces oxytocin receptor up-regulation in the amygdala and hypothalamus via an adenosine a2a receptor-independent mechanism. Pharmacol. Biochem. Behav. 119 (2), 72–79.
Zanos, P., Georgiou, P., Wright, S.R., Hourani, S.M., Kitchen, I., Winsky-Sommerer, R., et al., 2014b. The oxytocin analogue carbetocin prevents emotional impairment and stress-induced reinstatement of opioid-seeking in morphine-abstinent mice. Neuropsychopharmacology 39 (4), 855–865.
Zanos, P., Georgiou, P., Weber, C., Robinson, F., Kouimtsidis, C., Niforooshan, R., et al., 2017. Oxytocin and opioid addiction revisited: old drug, new applications. Br. J. Pharmacol. 175 (14), 2809–2824.